This document is a preprint of: M. Grieger, S. Boob and G. Fettweis, "Large Scale Field Trial Results on Frequency Domain Compression for Uplink Joint Detection," in Proceedings of IEEE Global Communications Conference 2011 (GLOBECOM 2012), Dec 2012. DOI:10.1109/GLOCOMW.2012.6477737

Large Scale Field Trial Results on Frequency Domain Compression for Uplink Joint Detection

Michael Grieger, Stefan Boob, Gerhard Fettweis
Technische Universität Dresden,
Vodafone Chair Mobile Communications Systems,
Email: {michael.grieger, stefan.boob, fettweis}@ifn.et.tu-dresden.de

***Abstract*—The spectral efficiency of cellular communication systems is limited by inter-cell interference. Especially cell edge users will experience bad performance. A potential remedy to inter-cell interference is joint signal processing on the base station (BS) side. In the cellular uplink the received signals of multiple BSs can be processed at a central node, referred to as joint detection (JD). Field trials of this technique verify large improvements in spectral efficiency and fairness which were initially proven in theoretical and simulation studies. Recent studies encourage that JD is even beneficial under stringent backhaul constraints which are likely to occur in real deployments. The general solution in case of limited backhaul capacity is based on the compression of exchanged signals. This paper presents the most significant design criteria of such compression algorithms for an LTE-Advanced system. We focus on the exchange of frequency domain IQ-symbols. The limits and potentials of a comprehensive system solution are evaluated using data from large scale field trials.**

I. Introduction

The spectral efficiency of today's cellular systems is limited by inter-cell interference. Especially, data rates for mobile users that are located at cell edges are drastically reduced by this effect resulting in a lack of fairness. Some of the current, most promising proposals, for an improved system setup consider the use of coordinated multi-point (CoMP) techniques for the uplink and downlink. Previous field trial (FT) publications such as [1] demonstrate that today's technology is ready to support these concepts.

The focus of this paper is joint detection (JD) for the cellular uplink which puts very challenging capacity and latency requirements on the backhaul network because it relies on the exchange of received signals. An early evaluation of backhaul requirements, based on system level simulations, was given in [2]. Theoretical analysis, on the other hand, promises great increases in spectral efficiency even under limited backhaul capacity [3]–[5]. These studies invoked rate-distortion theory in order to derive achievable rate solutions for JD under backhaul constraints and to optimize e.g. the distribution of compression bits over a certain number of parallel channels. Clearly, practical system design that incorporates JD under backhaul constraints poses many further interesting challenges and optimization problems. One task is the design of compression algorithms. The performance of multiple scalar and vector compression schemes for uplink JD were evaluated in [6] by assessing the post detection SINR in a small scale FT. It was shown that scalar compression already achieves a remarkable performance at about $4-5$ bit per real sample. In [7] the performance of JD was evaluated for time domain (TD) signal compression in a large scale FT. This approach, however, has multiple drawbacks, such as its inapplicability to dynamic base station (BS) clustering and an inherent overhead due to oversampling.

In the present paper, we consider compression of frequency domain (FD) symbols, which is shown to be the more flexible approach. First, we address multiple challenges such as the potential need to adapt the compression codebook according to the input distribution and the exploitation of antenna correlation. Based on this preliminary study, we propose a comprehensive design for FD BS signal exchange and evaluate this design using two sets of FT data. First we reuse the FT measurement data that was also used in [7] and compare TD and FD compression performance. In order to investigate the impact of additional parameters, especially the number of uplink data streams, we use new FT data of up to four user equipments (UEs) transmitting on the same resources. While the presented study of FD compression for JD is catered to an LTE-Advanced uplink, the results are certainly not limited to this particular system.

In the sequel, the measurement setup is described in Section II. A summary of the signal processing architecture is given in Section III, and details on compression algorithms are described in Section IV. FT results are presented in Section V. The paper is concluded in Section VI.

II. Field Trial Setup

In this section, we give an overview of the FT system used in order to lay the basis for the identification of practical signal processing challenges. The LTE-Advanced tested is located in downtown Dresden, a representative area of a medium-sized European city. Since it covers surroundings of very different building morphology, various propagation conditions can be tested which are of special interest for evaluation of fourth-generation (4G) systems. This includes interference conditions that are typical in frequency reuse one networks like LTE which is very beneficial for the development of advanced algorithms such as JD. BSs and UEs are implemented on prototype hardware. As mentioned previously, the basic physical layer procedures of the FT hardware are used in close compliance with the 3GPP/LTE standard (see e.g. [8]). This concerns mainly the control and data processing. However, as a major difference, OFDM instead of SC-FDMA

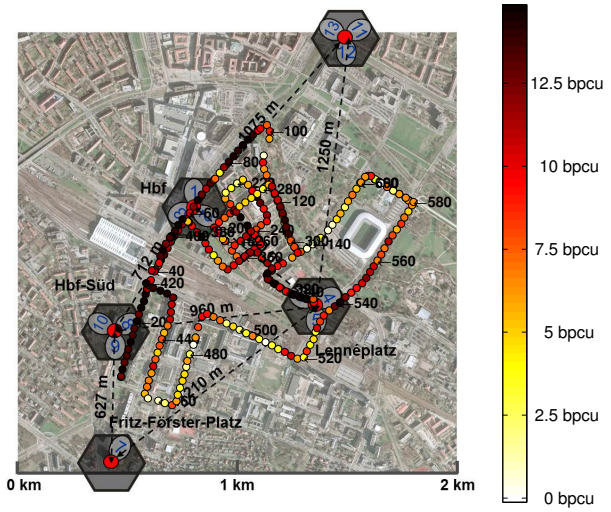

Fig. 1. Testbed Deployment of FT 2 and JD ($C = 3$) sum-rate of $K = 4$ Tx streams at measurement locations. Map data © Sandstein Neue Medien GmbH (http://stadtplan.dresden.de)

is used in the uplink. Time and frequency synchronization of BSs, which is required for joint signal processing, is done through GPS fed reference normals. Each BS is equipped with a two element, cross-polarized LTE antenna (58 degrees half-power beamwidth and 14 dBi gain). The UEs share the same resources in time and frequency. Employing one dipole antenna, they transmit a sequence of different modulation and coding schemes (MCSs). The signals received at all BSs are recorded for offline evaluation. Thus, the focus of the investigation is on physical layer evaluation.

The evaluation in Section V is based on two different FTs. In FT 1, the same FT measurement data of 16 BSs and $K = 2$ UEs as in [7] was used. We refer the reader to this publication for more information on the particular BS and UE settings. In FT 2, a setup of 13 BSs at 5 sites was used as depicted in Figure 1. In total four UE-antennas were mounted as a linear array with 33.6 cm($= 3\lambda$) distance on the roof of a measurement bus.

III. Signal Processing Architecture and Evaluation Concept

The general BS offline signal processing includes

- OFDM symbol timing and frequency synchronization
- demapping of reference and data symbols
- channel estimation
- noise variance estimation
- symbol equalization
- QAM symbol demapping and decoding

We concentrate on particular signal processing steps that are relevant for JD with FD compression of BS signals in the following since other steps were discussed in previous publications (e.g. [1], [7]). After OFDM symbol synchronization the cyclic prefix is removed and the received signals at all BSs is converted to the FD using an FFT. As a next step, reference and data symbols are separated. Channel estimation as well as noise variance estimation are performed based on the reference symbols transmitted on the 4th and 11th OFDM symbols of each transmit time interval (TTI). In total 11 data OFDM symbols are transmitted in each TTI. The received signal of each symbol on a single orthogonal frequency division multiplexing (OFDM) sub-carrier at BS m can be stated as

$$\mathbf{y}_m = \sum_{k=1}^{K} \mathbf{h}_{m,k} x_k + \mathbf{n}_m, \tag{1}$$

where $\mathbf{y}_m \in \mathbb{C}^{[N_{\text{bs}} \times 1]}$ is the signal received by N_{bs} antennas of BS m, $\mathbf{h}_{m,k} \in \mathbb{C}^{[N_{\text{bs}} \times 1]}$ denotes the channel gain from UE k to BS m, $x_k \in \mathbb{C}$ is a symbol transmitted by UE k, and $\mathbf{n}_m \in \mathbb{C}^{[N_{\text{bs}} \times 1]}$ denotes additive, uncorrelated noise of variance $\mathbf{S}_m^2 \mathbf{I}$. The channel vectors include UE transmit power due to the assumption of $E\{x_k x_k^H\} = 1$. If JD is used, a set of BSs in a cooperation cluster exchange their received signals to a central node, thus forming a network MIMO system. The set of BSs that form a cooperation cluster is denoted by $\mathcal{C}$ with elements $\{c_1 \dots c_C\}$, where the cooperation cluster size is denoted by $C = |\mathcal{C}|$. The corresponding transmission model for the cluster is given by

$$\mathbf{y}_{\mathcal{C}} = \sum_{k=1}^{K} \begin{bmatrix} \mathbf{h}_{c_1,k} \\ \vdots \\ \mathbf{h}_{c_C,k} \end{bmatrix} x_k + \mathbf{n}_{\mathcal{C}} + \mathbf{q}_{\mathcal{C}}, \tag{2}$$

where $\mathbf{y}_{\mathcal{C}} \in \mathbb{C}^{[N_{\text{bs}} C \times 1]}$ are the signals received by the C antennas of the cluster, and $\mathbf{n}_{\mathcal{C}}, \mathbf{q}_{\mathcal{C}} \in \mathbb{C}^{[N_{\text{bs}} C \times 1]}$ are noise and potential compression distortion respectively.

We consider conventional and JD of cluster sizes $C \leq 3$. A linear minimum mean square error (MMSE) detector is used. For conventional detection of UE k at BS m the filter matrix for a particular sub-carrier is given by

$$\mathbf{D}_{\text{biased}}^{[m,k]} = \hat{\mathbf{h}}_{m,k}^H \left(\sum_{\bar{k}=1}^{K} \hat{\mathbf{h}}_{m,\bar{k}} \hat{\mathbf{h}}_{m,\bar{k}}^H + \sigma_m^2 \mathbf{I} \right)^{-1}, \tag{3}$$

where $\hat{\mathbf{h}}$ are estimates of the channel. If the receive signals of all BSs in a cluster are available at a joint receiver, the biased MMSE filter for UE k is given by

$$\mathbf{D}_{\text{biased}}^{[k]} = \hat{\mathbf{h}}_{\mathcal{C},k}^H \left(\sum_{\bar{k}=1}^{K} \hat{\mathbf{h}}_{\mathcal{C},\bar{k}} \hat{\mathbf{h}}_{\mathcal{C},\bar{k}}^H + \Phi_{\mathbf{n}_{\mathcal{C}}\mathbf{n}_{\mathcal{C}}} + \Phi_{\mathbf{qq}} \right)^{-1}, \tag{4}$$

where $\hat{\mathbf{h}}_{\mathcal{C},k} = \left[\hat{\mathbf{h}}_{c_1,k}^T \ \cdots \ \hat{\mathbf{h}}_{c_C,k}^T \right]^T$, $\mathbf{h}_{c_i,k} = \left[h_{c_i,k}(1) \cdots h_{c_i,k}(N_{\text{bs}}) \right]$, $h_{c_i,k}(n_{\text{bs}})$ is the channel between UE k and the n_{bs}th antenna of BS c_i, and $\Phi_{\mathbf{n}_{\mathcal{C}}\mathbf{n}_{\mathcal{C}}} = \text{diag}\left[\text{diag}^{-1}\left(\sigma_{c_1}^2 \mathbf{I}\right) \cdots \text{diag}^{-1}\left(\sigma_{c_C}^2 \mathbf{I}\right) \right]$, and $\Phi_{\mathbf{qq}}$ is the covariance matrix of the compression noise which is explained in the following section. After equalization,

signal-to-interference-plus-noise ratios (SINRs) are estimated via an error vector magnitude approach, followed by soft demodulation. The demodulator output is fed into an LTE Rel. 8 compliant decoding chain.

IV. Frequency Domain OFDM Signal Compression

Compression is used for compliance with backhaul rate limitations. On the downside, compression causes distortion that limits throughput. In this work, compressed FD signals are exchanged, using an Fast Fourier Transform (FFT) before compression. This approach has several advantages compared to the exchange of TD signals which was applied in [7]. Uplink UEs typically do not transmit over the complete bandwidth. In our FT system, for example, the LTE 20 MHz mode is used which allows transmitting a total of 100 PRBs or $12 \cdot 100 = 1200$ sub-carriers. Out of these, only $N_{\text{PRB}} = 30$ PRPs (360 sub-carriers) are allocated to the FT UEs. Per TTI (1 ms) $N_{\text{data}} = 11$ OFDM symbols are used for data transmission. Thus, the symbol rate of the compression algorithm is $r_{\text{s}}^{\text{FD}} = 2(\text{real dimensions}) f N_{\text{bs}} \cdot 12 N_{\text{PRB}} \cdot 1000 N_{\text{data}} \frac{\text{real symbols}}{\text{s}}$. Assuming a $N_{\text{bs}} = 2$ this is a symbol rate of $r_{\text{s}}^{\text{FD}} = 15.84 \cdot 10^6 \frac{\text{real symbols}}{\text{s}}$, a significant reduction when compared to the exchange of the TD signal, where $r_{\text{s}}^{\text{TD}} = 2 N_{\text{bs}} f_{\text{s}} = 122.88 \cdot 10^6 \frac{\text{real symbols}}{\text{s}}$. Reasons for the large symbol rate for the TD signal are oversampling ($f_{\text{s}} = 30.72$ MHz instead of 20 MHz), the intrinsic exchange of control and pilot information and that r_{s}^{TD} does not scale with the cell load. Note that r_{s}^{FD} does not include the exchange of channel information. Instead, we assume perfect channel information at the joint detector. In practice, different compression algorithms can be used for data and channel information which is another benefit of FD compression. Presumably, the overhead for the exchange of channel information can be made small because time and frequency correlation can be exploited. Another benefit of FD compression is that it supports dynamic clustering, i.e. that different BSs are able to cooperate on different physical resource blocks (PRBs). We will address the most relevant aspects of FD compression the following paragraphs.

a) Location of Joint Decoder: We assume that the location of the joint decoder can be flexibly chosen depending on the channel conditions, but it is always placed at one BS of the cooperation cluster. Furthermore, we assume that the exchange of signals between BSs at the same site does not require the use of any backhaul. However, the signals of all $\tilde{C}$ remote BSs in $\mathcal{C}$ potentially need to be compressed in order to satisfy backhaul rate constraints. The set is these BSs is denoted by $\tilde{\mathcal{C}} = \{\tilde{c}_1, \ldots, \tilde{c}_{\tilde{C}}\}$.

b) Optimal Input Distribution: A quantization function maps input values from a partitioning of the input range to a set of output or reproduction values (or codebook). To minimize distortion, this mapping is optimized according to the probability distribution of the input signal which changes constantly due to time varying channels. The TD received signal power at the BSs is adjusted to the dynamic range of a 12 bit linear analog to digital converter (ADC) using an automatic gain control (AGC) amplifier. Thus, the TD signal has roughly constant power, and since it is the superposition of OFDM symbols and noise, its distribution is approximately Gaussian. Therefore, a fixed codebook is sufficient for the compression of the TD signal. The situation is more complex in the FD. The channel and therefore the input distribution is typically frequency selective. This issue can be solved using an FD-AGC. The received symbol at antenna n_{bs} of BS $\tilde{c}_i$ is multiplied by a gain that inverts the effect of the channel and noise for each sub-carrier and OFDM symbol before compression:

$$g_{\tilde{c}_i, n_{\text{bs}}} = \frac{1}{\sqrt{2}} \frac{1}{\sqrt{\sum_{k=1}^{K} \left| \hat{\mathbf{h}}_{\tilde{c}_i, k}(n_{\text{bs}}) \right|^2 + \sigma_{\tilde{c}_i}^2}}. \tag{5}$$

The sub-carrier and OFDM symbol index are omitted for the sake of brevity. We included the factor $\frac{1}{\sqrt{2}}$ to achieve that the variance of the real and imaginary part of the signal after FD-AGC is equal to one.

Since the symbols on each sub-carrier are a superposition of QAM symbols and Gaussian noise, they are non-Gaussian. Ideally, the codebook should be adjusted to each channel realization. Instead of following this complex approach, we first observe the loss that would occur when the codebook is optimized to a Gaussian input distribution instead which is equivalent to the relative entropy of both distributions [9, Section 2.3]:

$$D(P||Q) = \int_{-\infty}^{\infty} p(x) \ln \frac{p(x)}{q(x)}. \tag{6}$$

The relative entropy can be interpreted as a measure of the additional information that has to be exchanged over the backhaul if an input distribution of $p(x)$ is assumed while the actual distribution is $q(x)$. In a first evaluation, we look at an AWGN channel ($y = x + n$) where QAM of random data is used to generate x. Thus $q(y)$ is the distribution of noisy QAM values and $p(x)$ is a Gaussian distribution of the same variance. The differential entropy as a function of the SNR is depicted in Figure 2 for different QAM schemes. We see that the additional information is negligible at low SNR for any QAM order. The penalty starts to become significant at around 5 dB SNR for 4-QAM. However, today's cellular systems use adaptive modulation where typical SINR values for switching the modulation order in LTE are about 2 dB for 4/16-QAM and 10 dB for 16/64-QAM. In a cellular system, the received signal at each BS antenna is a superposition of useful signal, interference, and noise. Thus, the per antenna SINR is typically rather low (below 10 dB). Note that this discussion is only relevant for the uplink LTE-Advanced systems if an (optional) OFDM mode because SC-FDMA signals are approximately Gaussian in the FD.

c) Codebook Generation and Compression Algorithm: Different options for the generation of compression codebooks

This document is a preprint of: M. Grieger, S. Boob and G. Fettweis, "Large Scale Field Trial Results on Frequency Domain Compression for Uplink Joint Detection," in Proceedings of IEEE Global Communications Conference 2011 (GLOBECOM 2012), Dec 2012. DOI:10.1109/GLOCOMW.2012.6477737

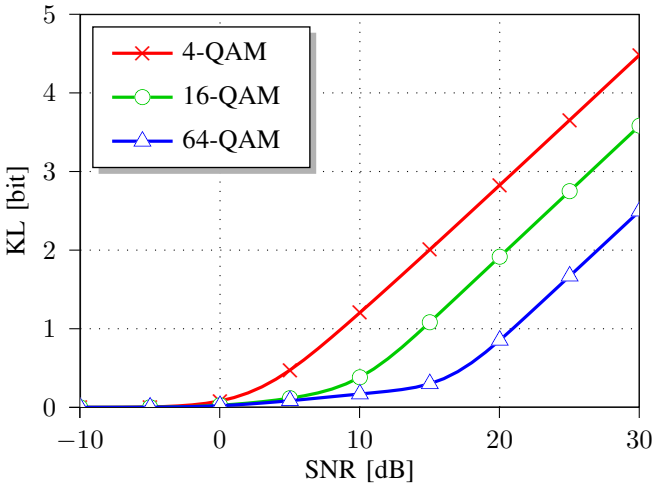

Fig. 2. Relative entropy between distribution of noisy QAM and Gaussian distribution

are discussed in [6]. We distinguish scalar and vector compression where the latter was shown to achieve a reduction of about $0.5-1$ bit per real sample (bprs) in the low backhaul regime, at the cost of a higher complexity. This gain comes from the exploitation of signal correlation due to non-orthogonal channel matrices and to optimized shaping of the codebook in multiple dimensions. However, the exploitation of signal correlation is also possible using an Eigenvector transformation (EVT) prior to scalar compression at a lower cost in terms of complexity. Using the singular value decomposition (SVD) of $\mathbf{H}_{\tilde{c}_i} = \left[\mathbf{h}_{\tilde{c}_i,1}, \ldots, \mathbf{h}_{\tilde{c}_i,K}\right]$, we can write

$$\mathbf{y}'_{\tilde{c}_i} = \mathbf{U}^H \mathbf{y}_{\tilde{c}_i} = \mathbf{U}^H \underbrace{\mathbf{U}\mathbf{S}\mathbf{V}^H}_{\mathbf{H}_{\tilde{c}_i}} \mathbf{x} + \mathbf{U}^H \mathbf{n} = \mathbf{S}\mathbf{V}^H \mathbf{x} + \tilde{\mathbf{n}}, \quad (7)$$

Since $\mathbf{x} = \begin{bmatrix} x_1 & \ldots & x_K \end{bmatrix}^T$ is uncorrelated, circular symmetric and $\mathbf{U}, \mathbf{V}$ are a unitary matrices, $\mathbf{V}^H\mathbf{x}$ and $\tilde{\mathbf{n}} = \mathbf{U}^H\mathbf{n}$ have unchanged statistical properties and are therefore i.i.d.. $\mathbf{S}$ is a matrix with $\min(K, N_{\text{bs}})$ singular values on the diagonal and $\mathbf{S}\mathbf{V}^H\mathbf{x}$ has lower power than $\mathbf{x}$ because of the removed correlation, which can be exploited for increased compression accuracy. If $K < N_{\text{bs}}$ only K elements of $\mathbf{y}'_{\tilde{c}_i}$ contain signal information leading to an even larger reduction of the backhaul rate because signal components that correspond to zero singular values are not exchanged at all.

We believe that the shaping gain alone does not justify the additional complexity of vector compression and thus use scalar compression after (potential) signal decorrelation. As described above, an FD-AGC is required, in order to account for power differences of orthogonal signal components in $\mathbf{y}'_{\tilde{c}_i}$. The scaling factor is $g'_{\tilde{c}_i,n_{\text{s}}} = \frac{1}{\sqrt{2}} \frac{1}{\sqrt{s_{n_{\text{s}}}^2 + \sigma_n^2}}$, where $s_{n_{\text{s}}}$ is the n_{s}th singular value of $\mathbf{H}_{\tilde{c}_i}$.

In summary, the signal prior to compression is

$$\mathbf{y}''_{\tilde{c}_i} = \mathbf{G}_{\tilde{c}_i} \mathbf{y}_{\tilde{c}_i} \quad (8)$$

if received signals are compressed directly after FD-AGC, and

$$\mathbf{y}''_{\tilde{c}_i} = \mathbf{G}'_{\tilde{c}_i} \mathbf{U}^H \mathbf{y}_{\tilde{c}_i} = \mathbf{G}'_{\tilde{c}_i} \mathbf{y}'_{\tilde{c}_i} \quad (9)$$

if an additional EVT is applied. In these equation, we used $\mathbf{G}_{\tilde{c}_i} = \text{diag}\left(\begin{bmatrix} g_{\tilde{c}_i,1} & \ldots & g_{\tilde{c}_i,N_{\text{bs}}} \end{bmatrix}\right)$ and $\mathbf{G}' = \text{diag}\left(\begin{bmatrix} g'_{\tilde{c}_i,1} & \ldots & g'_{\tilde{c}_i,N_{\text{bs}}} \end{bmatrix}\right)$

An algorithm for the determination of the MMSE distortion quantizer was established by Max and Lloyd. Optimal codebooks for Gaussian distributions can be efficiently expressed in tables. The values in these table can be matched to any Gaussian input by adding the mean and multiplying them by the standard deviation. Even though the input distribution of $\mathbf{y}''_{\tilde{c}_i}$ is not exactly Gaussian (see discussion above), we apply this approach in our work. The problem of finding the MMSE reproduction value in codebook $\mathbb{C}_{\text{b}}$ is

$$Q(y''_{\text{re/im}}) = \hat{y}'' = \min_{\hat{y}_i \in \mathbb{C}_{\text{b}}} d(y'', \hat{y}''_i) \quad (10)$$

where $y''_{\text{re/im}}$ is any real or imaginary part of the elements in $\mathbf{y}''$. The search can be implemented using a tree structured algorithm which is very efficient in terms of complexity [6]. The joint decoder reverts the FD-AGC and, potentially, the EVT in order to obtain

$$\hat{\mathbf{y}}_{\tilde{c}_i} = \left(\mathbf{G}_{\tilde{c}_i}\right)^{-1} \mathbf{U} \mathbf{y}''_{\tilde{c}_i}. \quad (11)$$

Clearly, this approach requires full channel knowledge at the joint decoder (which is required for JD anyhow).

d) Compression Distortion: Received signals of BSs that are not collocated with the joint decoder are compressed. The compression distortion of these signals needs to be considered in (4). Its mean square error (MSE) is

$$\sigma^2_{\mathbf{q}'',\tilde{c}_i,n_{\text{bs}}} = E\left[\left(\mathbf{y}''_{\tilde{c}_i}(n_{\text{bs}}) - \hat{\mathbf{y}}''_{\tilde{c}_i}(n_{\text{bs}})\right)^2\right]. \quad (12)$$

The compression distortion of all signals of BSs that are collocated with the joint decoder, i.e. those in $\mathcal{C} \setminus \tilde{\mathcal{C}}$, is zero. Thus, $\Phi_{\mathbf{q}''\mathbf{q}''}$ is a diagonal matrix (compression distortion is uncorrelated) with non-zero elements for all BSs in $\tilde{\mathcal{C}}$. Note that the MSE is computed before the FD-AGC is reverted. After re-doing the FD-AGC, we thus get a MSE per symbol and antenna. If decorrelation was not used, we get

$$\Phi_{\mathbf{q}\mathbf{q},\tilde{c}_i} = \mathbf{G}^{-1}_{\tilde{c}_i} \Phi_{\mathbf{q}''\mathbf{q}''} \mathbf{G}^{-1}_{\tilde{c}_i}, \quad (13)$$

which is a diagonal matrix. Thus, $\mathbf{q}$ is uncorrelated. If the received signal at $\tilde{c}_i$ was decorrelated before compression, the expression for the mean square error is

$$\begin{aligned} \Phi_{\mathbf{q}\mathbf{q},\tilde{c}_i} &= E\left[\mathbf{q}\mathbf{q}^H\right] = E\left[\mathbf{U}\left(\mathbf{G}'_{\tilde{c}_i}\right)^{-1} \mathbf{q}''\mathbf{q}''^H \left(\mathbf{G}'_{\tilde{c}_i}\right)^{-1} \mathbf{U}^H\right] \\ &= \mathbf{U}\left(\mathbf{G}'_{\tilde{c}_i}\right)^{-1} \Phi_{\mathbf{q}''\mathbf{q}''} \left(\mathbf{G}'_{\tilde{c}_i}\right)^{-1} \mathbf{U}^H. \end{aligned} \quad (14)$$

The compression noise is, thus, correlated.

V. Field Trial Results

We use two different FT setups for the evaluation of the compression algorithm. First, referred to as FT 1, we use the same FT data as used in [7]. The measurement route had a length of about 17 km/h, as depicted in [7, Figure 1]. It was traversed by the measurement car at a speed of about

This document is a preprint of: M. Grieger, S. Boob and G. Fettweis, "Large Scale Field Trial Results on Frequency Domain Compression for Uplink Joint Detection," in Proceedings of IEEE Global Communications Conference 2011 (GLOBECOM 2012), Dec 2012. DOI:10.1109/GLOCOMW.2012.6477737

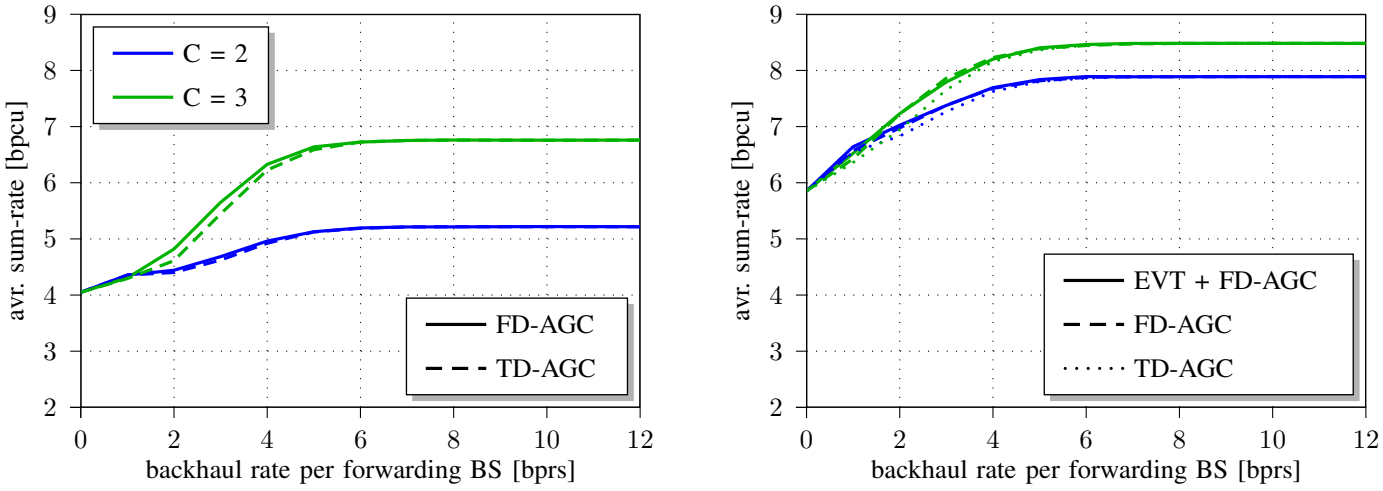

(a) $N_{\text{bs}} = 1$ (b) $N_{\text{bs}} = 2$

Fig. 4. Average sum-rate as a function of the backhaul rate per forwarding BS, real sample, and BS antenna for FT 1

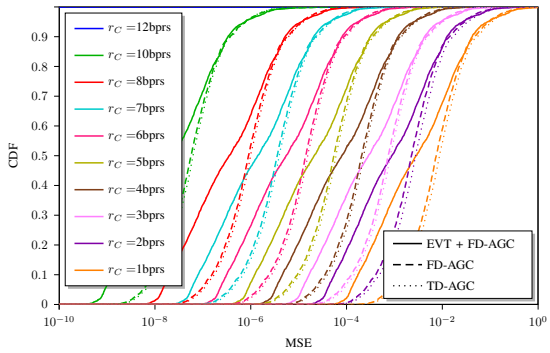

Fig. 3. MSE CDF for different compression algorithms in FT 1 ($N_{\text{bs}} = 2$)

6 km/h. In this FT $K = 2$ UEs were transmitting on the same resources. While the UEs were constantly transmitting switching cyclically through different MCSs, the received signal at the BSs was evaluated for a block of 40 ms every 10 s. This way we were able to determine the maximum rate of each UE for each measurement location as described in [7].

For both measurement setups, we formed cooperation clusters of C BSs that achieved the highest $\hat{\text{SNR}}_l^m$ at each measurement location l. While the BS with the largest $\hat{\text{SNR}}_l^m$ was chosen to be the joint detector, the BSs in $\tilde{\mathcal{C}}$ forwarded their received signal, after compression with rate r_{C}. In the following, we show results for different cooperation cluster sizes $C = 2$ and $C = 3$ and different compression rates $r_{\text{C}} = \{1, 2, 3, 4, 5, 6, 7, 8, 10, 12\}$ bprs using offline evaluation of the same measurement data set. First, we evaluate the MSE error of signal compression. We distinguish among three different options and evaluate their performance in terms of

1) FD-AGC and EVT (only for $N_{\text{bs}} = 2$) before compression.
2) compression includes FD-AGC before compression.
3) only TD-AGC before compression.

The use of decorrelation reduced compression distortion significantly. Channel realizations typically have one large and one smaller singular value, and since compression distortion is proportional to power the signal component that corresponds to the smaller singular value is less distorted. Thus, we see that about half of the MSE values are strongly reduced through decorrelation while the other half is not reduced. Note that decorrelation will often lead to signals of very unequal power (for badly conditioned channels). Such signals would, ideally, be compressed with different resolution; higher compression bit rate for the stronger signal. Unfortunately, algorithms which find an throughput optimal compression rate distribution are very complex [4]. An easier approach would be to minimize the overall MSE which leads to a water puring solution [9]. In this work, however, we chose to compress all signals with the same rate for simplicity. This solution has the clear practical benefit that the total compression rate is fixed and does not depend on the channel realization. The use of FD-AGC alone reduces average MSE only marginally.

Next, we compare achievable user rates of conventional and JD for different compression rates. The case when all BSs in the cooperation cluster $\mathcal{C}$ are located at the same BS is referred to as intra-site joint detection which, in FT] 1 occurs in about 30 % of the locations for $C = 2$. Three cases are distinguished for $C = 3$: either all three BSs are at the same site (intra-site JD) which was the case at 10% of the locations; the joint decoder was collocated with one BS in $\mathcal{C}$, or the joint decoder was located at a separate site. Collocating the joint decoder with other BSs in $\mathcal{C}$ reduces the backhaul requirements and avoids compression distortion of the exchanged signal. Ideally, the location of the joint decoder would be optimized taking all these options into account. We leave this option for future work and observe the sum-rate $r_{\text{sum},l} = \sum_{k=1}^{K} r_{kl}$ where r_{kl} is the rate of UE k at location l. The average sum-rate (over all locations) is shown in Figure 4. For the case of single antenna BSs ($N_{\text{bs}} = 1$) JD increases the rate from 4 bprs to 5.2 bprs for a cluster size of $C = 2$ (blue curves) and to

6.8 bprs for $C = 3$ (green cluves). Since both UEs are located in close vicinity, transmission on the same resources causes strong mutual interference which would result in very low data rates for conventional linear detection especially at single antenna BSs. For a fairer comparison, we emulate the case of only a single UE transmitting by canceling the interference of the other UE as described in [7]. Even though Figure 4(b) shows that the achieved sum-rate of conventional detection can be strongly increased using $N_{\text{bs}} = 2$ because interference can be reduced using spatial filtering, the gains of JD are still significant. However, it has to be noted that the total backhaul rate is multiplied by N_{bs}. Figure 4 also compares the performance of different compression algorithms. While the use of a FD-AGC gives some gains, decorrelation through EVT is only beneficial in the very low backhaul rate. This would have been different for $K < N_{\text{bs}}$ because an EVT would allow reducing the dimension of the received BS signals.

Figure 4 shows that a backhaul rate of more than 6 bprs does not increase the gain of JD. It could be expected that a higher backhaul rate could be useful if more UEs transmit on the same resources, since a higher number of transmitted data streams would superimpose at the receiver. In order to evaluate this aspect, another FT was done in which four UEs were carried on a measurement bus, a setup which could represent the feeder link of a moving relay as presented e.g. in [10]. The UE antennas were placed on the roof of the bus in a distance of 33.6 cm. The UEs were configured in a way that either one, two, three, or four were transmitting on the same resources while all other were silent ($K = 1, 2, 3, 4$). The setup is depicted in Figure 1 which also indicates the achieved sum-rate at each measurement for $N_{\text{bs}} = 2$ and $K = 4$. The average sum-rate for different K and C is shown in Figure 5. While the gain of JD is very small for $K = 1$ because no spatial multiplexing gain can be achieved, we see that for $C = 2$ either $K = 2$ or $K = 3$ is optimal while $K = 3$ achieves the best performance for $C = 3$. For any K, we see that increasing the backhaul rate above 6 bprs is again not beneficial.

VI. Conclusions

We have observed the performance of JD under limited backhaul rates. We discussed different design criteria for compression algorithms which were then evaluated in urban cellular FTs. We showed that the assumption of a Gaussian compression codebook achieves good performance for the compression of OFDM signals. The performance can be improved using FDAGC or decorrelation of antenna signals for which we presented signal processing schemes. However, the FT evaluation showed that the gains of these techniques are very limited for the observed setups. We have also seen that a backhaul rate above 6 bprs is not beneficial even if up to four data streams were transmitted at the UEs.

Acknowledgment

Part of this work has been performed in the framework the ICT project ICT-5-258512 EXALTED, which is partly funded by the European Union. The author Michael Grieger would like to acknowledge the contributions of his colleagues in EXALTED, although the views expressed are those of the authors and do not necessarily represent the project. Further, this work would not have been possible without support from Patrick Marsch, Ainoa Navarro Caldevilla, Walter Nitzold, Sven-Einar Breuer, Vincent Kotzsch, and Eckhard Ohlmer.

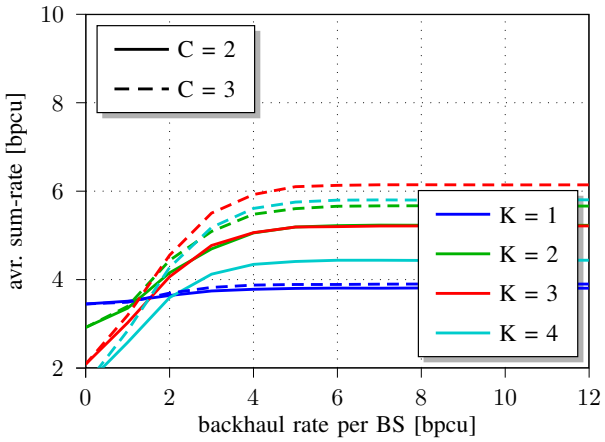

Fig. 5. Average sum-rate for different number of data streams K and cooperation cluster sizes C as a function of the backhaul rate per forwarding BS ($N_{\text{bs}} = 2$), real sample, and BS antenna for FT 2.

References

[1] M. Grieger, P. Marsch, and G. Fettweis, "Large Scale Field Trial Results on Uplink CoMP with Multi Antenna Base Stations," in *IEEE Vehicular Technology Conference, 2011. VTC 2011-Fall*, 2011.

[2] C. Hoymann, L. Falconetti, and R. Gupta, "Distributed uplink signal processing of cooperating base stations based on IQ sample exchange," in *Proceedings of IEEE Int. Conf. on Comm. (ICC'09)*, Dresden, Germany, June 2009.

[3] P. Marsch and G. Fettweis, "Uplink CoMP under a Constrained Backhaul and Imperfect Channel Knowledge," *IEEE Transactions on Wireless Communications*, vol. 10, no. 6, pp. 1730–1742, Jun. 2011.

[4] A. Del Coso and S. Simoens, "Distributed compression for mimo coordinated networks with a backhaul constraint," *Wireless Communications, IEEE Transactions on*, vol. 8, no. 9, pp. 4698 –4709, september 2009.

[5] D. Gesbert, S. Hanly, H. Huang, S. Shamai Shitz, O. Simeone, and W. Yu, "Multi-cell MIMO cooperative networks: A new look at interference," *IEEE Journal on Selected Areas in Communications*, vol. 28, no. 9, pp. 1380–1408, 2010.

[6] M. Grieger, P. Helbing, P. Marsch, and G. Fettweis, "Field trial evaluation of compression algorithms for distributed antenna systems," in *34th IEEE Sarnoff Symposium*, Princeton, USA, 2011.

[7] M. Grieger and G. Fettweis, "Large scale field trial results on time domain compression for uplink joint detection," in *IEEE 22nd International Symposium on Personal, Indoor and Mobile Radio Communications (PIMRC '11)*. IEEE, 2011.

[8] 3GPP, *Further Advancements for E-UTRA: Physical Layer Aspects*, Mar. 2010, tR 36.814 v9.0.0.

[9] T. M. Cover and J. A. Thomas, *Elements of Information Theory 2nd Edition*. Wiley-Interscience, July 2006.

[10] M. Sternad, M. Grieger, R. Apelfröjd, T. Svensson, D. Aronsson, and A. B. Martinez, "Using Predictor Antennas for Long-Range Prediction of Fast Fading for Moving Relays," in *IEEE Wireless Communications and Networking Conference (WCNC'12)*, 2012.